

EXPERIMENTAL ANALYSIS OF PARABOLIC TROUGH COLLECTOR SYSTEM WITH MULTIPLE RECEIVER GEOMETRIES AND REFLECTIVE MATERIALS

by

**Muzumil ANWAR^a, Ahmad WASIM^{a*}, Muzaffar ALI^b,
Salman HUSSAIN^a, and Mirza JAHANZAIB^a**

^a Industrial Engineering Department, University of Engineering and Technology, Taxila, Pakistan

^b Mechanical Engineering Department, University of Engineering and Technology, Taxila, Pakistan

Original scientific paper

<https://doi.org/10.2298/TSCI191202216A>

Solar parabolic trough collector systems provide an attractive solution especially for solar thermal power generation. The performance of these systems significantly depends on receiver geometries. Therefore, in the current study, an experimental analysis has been performed using three different receiver geometries along-with two reflective materials. These receiver geometries include: simple tube (reference geometry A), receiver tube with straight absorber plate (geometry B), and receiver tube with curved absorber plate (geometry C), whereas, the reflective materials include: aluminum and stainless steel. The experimentation was performed under subtropical climate conditions of Taxila, Pakistan. From experimentation, it was identified that peak heat gain obtained from receiver geometries C and B were 71%, and 30% higher as compared to the reference geometry A, respectively. The, thermal efficiency of the system with geometry A was 20%, geometry B was 28%, and geometry C was 34%. Furthermore, two reflective materials i.e. aluminum and Stainless steel were used on geometry C which yielded best results for further parabolic trough collector performance analysis. It was observed that peak thermal efficiencies were 34.8% and 31% with aluminum and stainless steel as reflector materials. The results indicated that aluminum reflector was approximately 12% efficient as compared to stainless steel reflector. The results will help to cultivate the advantages of innovative receiver geometries and alternative reflective materials.

Key words: *parabolic trough collector, receiver geometry, reflector coating, performance assessment, thermal efficiency*

Introduction

The traditional way of obtaining energy from burning fossil fuels needs to be minimized in order to reduce the greenhouse effects, global warming and disastrous changes in climate [1]. Currently, fossil fuels and nuclear energy are covering 91% of world energy demand, whereas only 9% are covered by renewable energy resources [2]. Renewable sources can be utilized alternatively which are available in abundant quantity. The potential of these renewable energy resources is evident from the fact that they can meet 140 times the current global energy demands. However, only 0.1% of renewable energy resources are being utilized [3]. Among different renewable energy resources, solar energy is considered to be one of the most significant resource for power generation at industrial and domestic sectors [4].

* Corresponding author, e-mail: wasim.ahmad@uettaxila.edu.pk

The average, fig. 1, sunshine days are approximately 300 with 7-8 sunshine hours and average direct normal irradiance of 6-6.5 kWh/m² daily [3]. Similar solar conditions are observed in solar energy rich countries around the globe. Therefore, the current research has the potential to harvest energy for wide range applications around the globe.

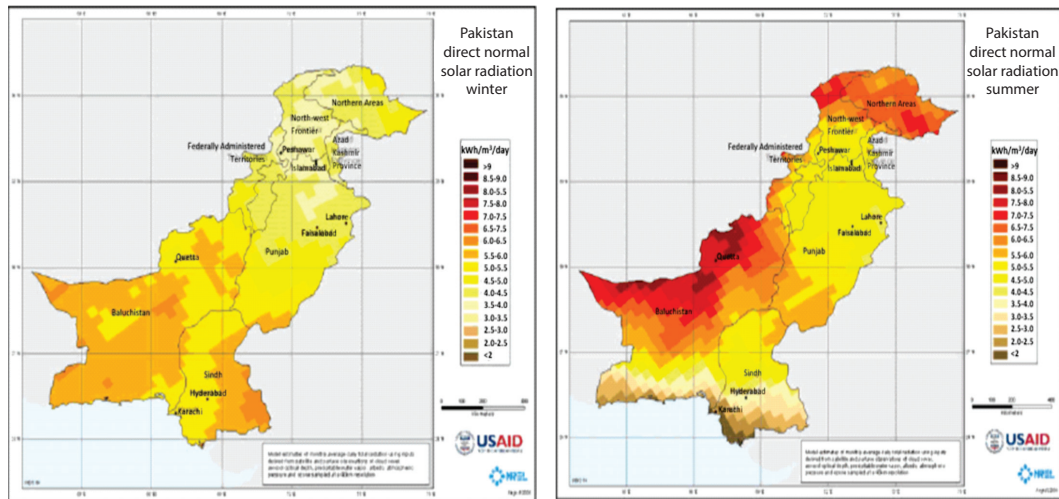


Figure 1. Solar radiation map of Pakistan during winter and summer [5]

There are three primary technologies to harness solar energy including photovoltaics, concentrating solar collectors and solar heating and cooling system. Out of these technologies, concentrating solar collector is one of the widely used techniques for research application. Different types of concentrating solar collectors have been developed by researchers including flat plate collectors, compound parabolic collectors, vacuum collectors, linear fresnel reflectors, parabolic trough collectors (PTC), heliostat field collectors and parabolic dish reflectors. Out of these solar collectors, PTC is found to be one of the most feasible solutions as it offers high temperature output and rapidly achieve high temperature of 60-400 °C [6-8]. Many research studies have been performed to enhance the thermal efficiency, heat absorption capacity and temperature of heat transfer fluid (HTF) flowing through receiver tube of PTC systems. This has been achieved by changing either geometries or area of the receiver tube. For example, Gandhi *et al.* [9] experimented on the alternative receiver tube geometries. They used stepped and uniform receiver tube geometries and performed the comparative analysis to identify the best option. The results indicated that stepped receiver tube was better with 5.41% improvement in outlet temperature. This was due to the fact that concentration ratio increased which lead to higher outlet temperature. Huai-Zhi *et al.* [10] numerically investigated the heat transfer mechanism on outward convex corrugated tube geometry. Reynolds stress transport model was used to analyze the stresses induced on fluid-flowing through receiver tube which ultimately effects on the heat transfer rate. The authors observed 8.4% improvement in heat transfer coefficient with the application of corrugated geometrical shape of receiver tube. Daabo *et al.* [11] performed comparative analysis of conical, spherical and cylindrical shaped receiver geometries. It was identified that conical shaped receiver geometry achieved higher efficiency of 77.05%, while the efficiencies obtained from cylindrical and spherical geometries were 69% and 63%, respectively. The reason behind higher efficiency was less radiative heat losses in conical receiver geometry as compared to cylindrical and spherical shaped geometries. Demagh *et al.* [12]

performed numerical analysis on s-curve sinusoidal shaped receiver geometry for heat transfer enhancement of PTC system. The research was based on the fact that Nusselt number increases with increase in number of curves which ultimately enhance the friction of fluid and thereby increase the fluid temperature. The results indicated that fluid friction increased by 40.8% with the application of sinusoidal geometry of receiver tube. Instead of changing the receiver tube geometry, Kumar and Shukla [13] designed helical coil solar cavity receiver to investigate the receiver tube performance of PTC. The results indicated that thermal losses were reduced which yielded 85% thermal efficiency. In addition changing geometries of receiver tube, researchers have investigated the effects of adding inserts on the receiver tube. For example, Bellos and Tzivanidis [14] compared the results of twisted tape inserts, perforated plate inserts and internally finned absorbers with smooth absorber. It was identified that the efficiency as high as 2.1% with non-evacuated and 1.6% with evacuated collectors was achieved by using internally finned absorber. In comparison, the perforated plate inserts and twisted tape inserts achieved efficiencies of 1.8% and 1.5%, respectively, for the non-evacuated collector and up to 1.4% and 1.2%, respectively, for the evacuated collector. Jaramillo *et al.* [15] used twisted tape inserts inside receiver tube and observed 2% increase in thermal efficiency with the addition of inserts. Contemporarily, Huang *et al.* [16] numerically analyzed the effects of dimples, protrusions and helical fins on the outer surface of receiver tube. The results indicated that receiver tube having dimples fins on outer surface of tube provides better heat transfer performance than the other two geometries. Bellos *et al.* [17] identified the effects of turbulators like inserts and internal fins or tube dimples on thermal efficiency of receiver tube. It was reported that internal fins resulted in 1.10% increase in thermal efficiency. The research also employed nanofluids which resulted in thermal efficiency enhancement of 0.76%. The overall efficiency enhancement of the system was observed to be 1.54%.

Number of researchers also worked on outer area of receiver tube with the objective to enhance the heat transfer rate and thermal efficiency of PTC system. For example, Razmmand and Mehdipour [18] observed the effects of three different coatings (titanium carbide, black chromium, and nickel) on stainless steel absorber tube. The maximum efficiency was reported with titanium carbide coating. Medina *et al.* [19], on the other hand, focused to increase the area of absorber pipe. Rectangular shaped absorber plate and curved shaped absorber plate were attached on the outer surface of the absorber pipe. It was identified through simulation study that curved profile was 25-28% more thermally efficient than rectangular profile [11].

Other than receiver geometry and area, the performance of PTC is also influenced by different reflective materials. These materials aid to reflect the maximum amount of solar flux from the surface of PTC to the absorber pipe. Higher specular reflectance for radiation in solar spectrum is the most desirable property for these materials [20]. For instance, black silver colored glass covered with several protective coatings has higher specular reflectance than the glass without coatings. Alternative reflective mirrors with better reflectance and strengths features are under research from last many decades. For example, Kaczor *et al.* [21] used different mirror curvatures to study the focus effects of solar radiations. Similarly, Sadaghiyani *et al.* [22] changed the curves of mirrors by incorporating linear and convoluted geometries. The modified reflectors resulted in enhancement of outlet temperature and thermal efficiency of compound parabolic concentrators. Bellos and Tzivanidis [23] used radiation shield as a second reflector for the absorber tube and achieved 0.90% thermal efficiency enhancement. Arasu *et al.* [24] used flexible solar flex foil as a reflective material and experimentally observed the thermal efficiency of the PTC system. The results indicated 47% increase in thermal efficiency. Muthu *et al.* [25] and Macedo-Valencia *et al.* [26] used aluminum reflector, whereas, Noman *et al.* [27] and Iqbal *et al.* [28] deployed stainless steel reflector in their experimental set-ups.

Keeping in view the relevant literature on numerical and experimental models of parabolic trough system, it is identified that limited experimental research work has been carried out on receiver tube geometries. Therefore, in current research, three different receiver geometries in the form of black body absorber plates have been designed. The efficiencies of these geometries have been experimentally analyzed. In addition, thermal assessment of PTC has been performed with different reflector materials *i.e.* aluminum and stainless steel in sub-tropical climate region of Taxila, Pakistan.

System description

Schematic diagram of PTC system is shown in fig. 2. It consists of solar collector, storage tank, pump to circulate water, temperature sensors for measuring temperature at inlet and outlet of receiver tube, digital pyranometer to record global radiations, flow sensor to set the flow rate of HTF and data acquisition system (DAS) for recording the data after every five minute from 9:00 a. m. to 5:00 p. m. The solar radiations falling on the surface of PTC get reflected and fall on the focal point of the receiver tube. Three different geometries of receiver pipe have been analyzed and shown in fig. 2. These geometries include

- simple receiver tube (Configuration A),
- receiver tube with straight absorber plate (Configuration B), and
- (receiver tube with curved absorber plate (Configuration C).

The detailed description of tubes nomenclature and PTC materials has been provided below.

Experimental set-up

The developed PTC system was installed at University of Engineering and Technology Taxila Pakistan (Latitude: 33°46'01.5" North, Longitude: 72° 49'37.4" East and 548.95 m above sea level). The PTC was set at axial position of north – south to allow the system to absorb maximum solar radiations in the east – west direction. As already explained, the system consists of three different absorber geometries A, B, and C. In all these geometries, the receiver tube was made of copper pipe having outer diameter of 25 mm. The black body absorber plates, on the other hand, were made of tin having width and thickness of 123.8 mm and 2 mm, respectively as shown in figs. 3(a) and 3(b).

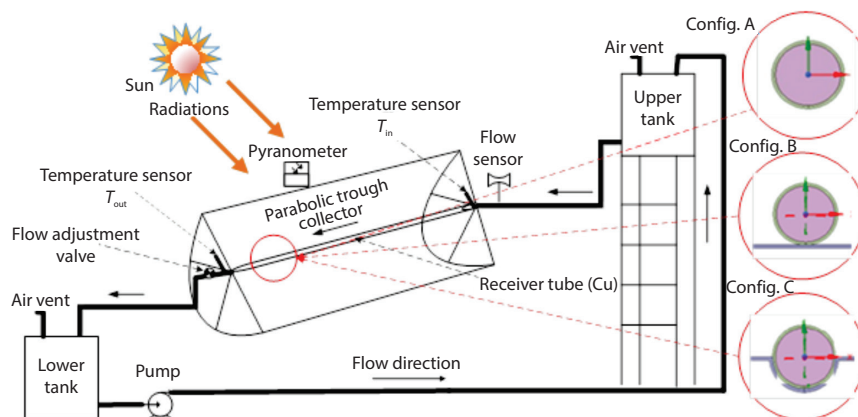


Figure 2. Schematic diagram of PTC system; (a) simple receiver tube, (b) receiver tube with straight absorber plate, and (c) receiver tube with curved absorber plate

Tin has been selected due to its low toxicity level, high resistance to corrosion and malleable with ductile nature [29]. To enhance the efficiency of tin absorber plate, it was made blackbody by coating diamond powder through heat treatment process at 200 °C using electric furnace. The absorptivity of absorber plate after treatment of coating with diamond powder was 0.93. To avoid convection heat loss with minimum climate effects, receiver tubes were covered within specially designed acrylic casing, fig. 3(c). Special care was taken to make the system airtight. Acrylic material was used for casing due to its comparable transparency (93%) with glass tube at low cost. Therefore, it was best alternate against glass tubes [25]. The installation of receiver tube with absorber plate inside the acrylic box has been shown in figs. 3(d)-3(f). The parabolic curve shaped trough was manufactured with two distinctive reflector materials namely: stainless steel and aluminum. The water was used as HTF which was made to flow through mild steel pipes. Positive displacement water pump and water tanks were used to circulate and store water in the system. The overall installed experimental system has been shown in fig. 4. The specifications of PTC system have been provided in tab. 1.

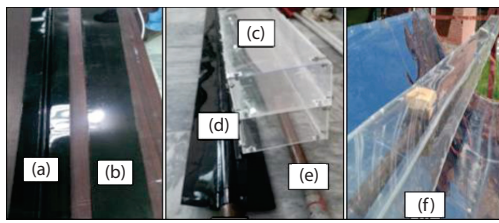


Figure 3. (a) Circular absorber plate, (b) straight absorber plate, (c) acrylic box casing, (d) absorber plate attached with receiver tube, (e) receiver tube, and (f) fabricated assembled receiver installed in experimental set-up

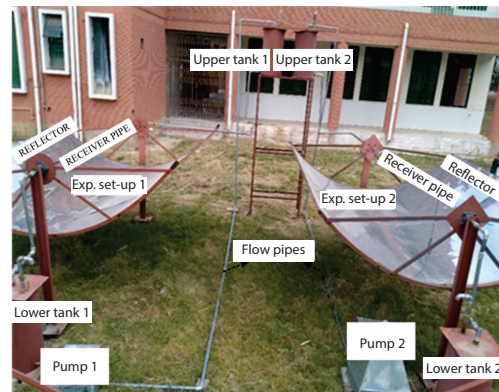


Figure 4. Experimental set-up

Experimental procedure, instrumentation, and measurements

In this research study, thermal performance of receivers pipe was experimentally analysed with three different receiver geometries *i.e.* A, B, and C alongwith two different reflective coatings *i.e.* aluminum and stainless steel, under actual climate conditions. Each system configuration (geometries A, B, and C and reflective coatings) have been tested and examined for 15 days between 9:00 a. m. to 05:00 p. m. during the months of May 2019 to June 2019. To accommodate all system configurations under similar conditions and to remove biasness, two experimental set-up having same specifications were modified and arranged

Table 1. Specifications of PTC

Specification	
Length of PTC, L	3.04 m
Aperture width of PTC, W_{apr}	2.65 m
Depth of PTC	0.66 m
Focal length of PTC	0.66 m
Aperture area, A_{apr}	8 m ²
Rim angle	90°
Outer diameter of receiver tube, d_o	0.025 m
Inner diameter of receiver tube, d_i	0.022 m
Outer surface area of receiver tube, A_r	0.239 m ²
Thickness of absorber plates	0.002 m
Area of straight absorber plate	0.37 m ²
Area of curved absorber plate	0.44 m ²
Concentration ratio, C_r	33.2
Mass-flow rate, \dot{m}	0.018 L/s
Specific heat of Cu, C_p	385 J/kgK

alternatively on daily basis in a commutative way (A-B, B-C, C-A). This arrangement was repeated for 15 days to ensure that each configuration was examined under the same operating conditions and averaged data was used at the end. Moreover, the effects of climate fluctuations were minimized by considering the data of only those 15 days when the full days was sunny and there was very slight difference in terms of radiations. To evaluate the performance of receiver geometries A, B, and C, stainless steel reflective coating was used.

At the start of experimentation, all pumps were switched on and upper tanks were filled with water. Once the tanks were filled, the inlet flow control valve was operated and a uniform flow of HTF was maintained with the help of flow sensors. Flow sensors (model: SEN-HZ21WA) having range of 1-30 Lpm with accuracy of $\pm 3\%$ were used at inlet of each of the receiver pipe. The system's zero leakage was ensured before the start of readings. The pressure drop was also measured randomly to ensure smooth flow-rate of HTF. Since the non-tracking PTC were used in this research, therefore, global radiation was measured directly for performance assessment of solar collector. These global radiation at site were measured after every hour through pyranometer (model: TM-207, range up to 2000 W/m^2 , accuracy $\pm 10 \text{ W/m}^2$ or $\pm 5\%$). Temperatures were measured through temperature sensors (model: DS18B20, temperature range -55 - 200°C , accuracy $\pm 0.5^\circ\text{C}$) installed at various locations including inlet and outlet of receiver pipe and outlet and inlet of supply and storage tanks, respectively. Ambient temperature was also measured through the same type of temperature sensor (model: DS18B20). Wind speed was measured through anemometer (model: 407119_A, range 0.2 - 17.0 m/s , accuracy $\pm 5\%$). The readings of system temperature, ambient temperature, flowrate, and wind speed were recorded after every five minutes. For this purpose, DAS was used. The calibration of all sensors was ensured before their installation. Furthermore, the instrument wirings were adequately shielded to ensure the signal noise reduction. The mass-flow rate of absorbent flowing through the receiver tube was kept constant during all experimentation. There was negligible shadowing effect of absorber plates on collector surface as the axis of collector was positioned at N-S axis and this arrangement ensures minimum shadowing effect [30]. Although the area of receiver tube attached with absorber plate was increased by 0.13 m^2 . However, this increase in area is negligible as compared to large reflector surface having aperture area of 8 m^2 and 2.65 m width.

Performance indicators

Optical efficiency of PTC is the ratio of energy absorbed by receiver to the energy projected on collector's aperture. It depends upon the geometry of reflector and material properties of reflector in terms of reflectance, absorptance, and transmittance. Equation (1) can be used to calculate the optical efficiency [31]:

$$\eta_0 = \rho \alpha \tau \gamma [(1 - A_f \tan \theta) \cos \theta] \quad (1)$$

where θ is the angle of incident which can be determined [32]:

$$\cos \theta = \sqrt{\cos^2(\theta_z) + \cos^2(\delta) \sin^2(w)} \quad (2)$$

Thermal efficiency of PTC is the ratio of heat gain by the absorbent in the receiver pipe and heat transfer to the trough through sunlight. Thermal efficiency at any instant can be calculated [33]:

$$\eta = \frac{Q_{\text{gain}}}{Q_{\text{rad}}} \quad (3)$$

Heat transfer through radiation between the receiver and sky, Q_{rad} can be expressed [34]:

$$Q_{\text{rad}} = GA_{\text{apr}} \quad (4)$$

Heat gain by the receiver due to incident sunlight energy can be calculated [33]:

$$Q_{\text{gain}} = \dot{m}C_p(T_{\text{out}} - T_{\text{in}}) \quad (5)$$

Equation (3)-(5) can thus be used to calculate the thermal efficiency [33]:

$$\eta = \frac{Q_{\text{gain}}}{Q_{\text{rad}}} = \frac{\dot{m}C_p(T_{\text{out}} - T_{\text{in}})}{GA_{\text{apr}}} \quad (6)$$

Results and discussion

Climate Variations

The average variation in global radiation during experimentation period has been shown in fig. 5. It can be seen from the figure that average fluctuation was approximately 5% during this period. Maximum solar radiation of 1214 W/m² was observed at 1:00 p. m. On the other hand, least average solar radiations (800-890 W/m²) were observed at start and end of the day. Figure 6 presents the average variation in ambient temperature at different times of the day during the period under study. It can be seen that the ambient temperature varies between 32 -38 °C.

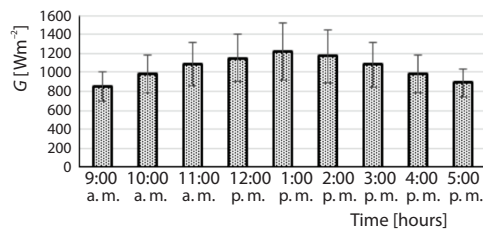


Figure 5. Average global radiation

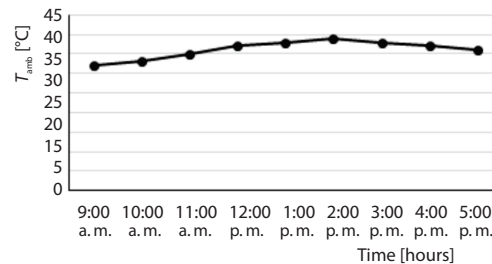


Figure 6. Average ambient temperature

Analysis of receiver geometries

Temperature gain, ΔT , and thermal efficiency, η , have been analyzed for three receiver geometries A, B, and C. The results of temperature gain, ΔT , have been presented in fig. 7. It is clear from the figure that the highest temperature gain, ΔT , of 74 °C was achieved for receiver geometry C as compared to highest temperature gain of 62 °C and 52 °C obtained for geometry B and A, respectively. Geometry C and B resulted in high temperature gain as compared to reference geometry A because these geometries were made with black body absorber plates which increases the heated region of receiver tube. Geometry A, on the other hand, was not attached with any blackbody absorber plate. Furthermore, it can be observed that 42.30% and 19.23% higher temperature gain was achieved for geometry C and B, respectively, as compared to reference geometry A. This is due to the fact that geometry C was attached with absorber plate having 50% additional cross-sectional area of receiver pipe, geometry B was in point contact with receiver pipe, whereas, geometry A had no absorber plate.

Figure 8 illustrates the results of thermal efficiency, η , with time. It can be seen from the fig. 8 that thermal efficiency kept increasing with the passage of time until mid of the

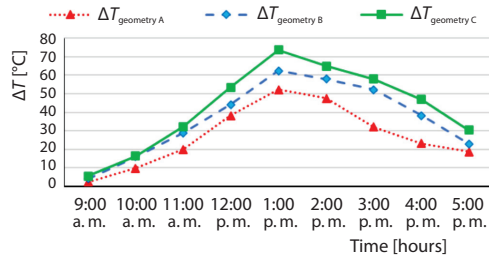


Figure 7. Variations in temperature gain

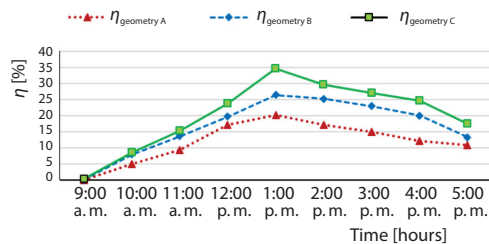


Figure 8. Variations in thermal efficiency

day. The thermal efficiency at the start of the day was almost 0% which increased to its maximum value at 1:00 p. m. when solar radiation reached at its peak, after this it started to decrease. Receiver geometry C achieved maximum thermal efficiency of 34.6%, while geometry B obtained peak thermal efficiency of 27.5% at 1:00 p. m. with reference to the simple geometry A having maximum thermal efficiency 20%. Because of significant impact of black body absorber plates, receiver tube having more area of contact with absorber plate resulted in more heat transfer through the fluid-flowing in receiver pipe. The highest thermal efficiency of geometry C was 71% more than reference receiver geometry A, whereas, the peak thermal efficiency of geometry B was 30% greater as compared to reference geometry A.

Analysis of thermal efficiency vs global radiation

The experiments were performed at Taxila, Pakistan which has a specific climate condition. To generalize the data for other regions, thermal efficiency vs. global radiation analysis has been performed, fig. 9. This will aid to identify the achievable efficiency with reference to radiations falling on PTC. This analysis will be useful for the regions whose incident radiations are near to values of radiation falling at the experimental location. It can be observed from the figs. 9(a)-9(c) that at lowest 850 W/m² radiation, thermal efficiencies of the system having receiver geometry A, B, and C were 10.74%, 13.24%, and 17.52%, respectively. Comparatively, the thermal efficiencies of receiver geometry A, B, and C were 19.91%, 27.5 %, and 34.21%, respectively, with reference to the peak value of radiation 1214 W/m² falling on the surface of PTC. It is clearly evident from the figure that in configuration C, thermal efficiency is more affected with the change of radiation intensity followed by configuration B and A. It is also evident from the figure that due to high sensitivity to radiation, configuration C results in higher fluctuation in thermal efficiency around mean value as compared to configuration B and A. This is due to the fact that larger contact area of absorber plate attached with receiver tube leads to better heat transfer rate which ultimately results in increased temperature of fluid-flowing through the system. Although the achieved thermal efficiency appears to be very low, however, it is pertinent to mention that the achieved values are comparable with other published studies in same region [30, 31]. For the current research, low cost acrylic box has been deployed instead of vacuum tubes. Vacuum tubes yield high thermal efficiencies due to minimum heat losses as perfect sealing can be ensured. In contrast, the present study used acrylic box manufactured which resulted in thermal losses. Furthermore, nanofluids are used to increase the thermal efficiency whereas the present study employed water HTF as the focus of the study was to give a cost-effective solution. Moreover, the calculation of heat gain by using eq. (5) shows that mean useful heat achieved from geometry A, B, and C were 200 W, 250 W, and 300 W, respectively, which are competitive with similar studies. Mean thermal efficiency obtained from geometry A, B, and C were 15 %, 20 %, and 28 %, respectively, are also comparable with other published studies.

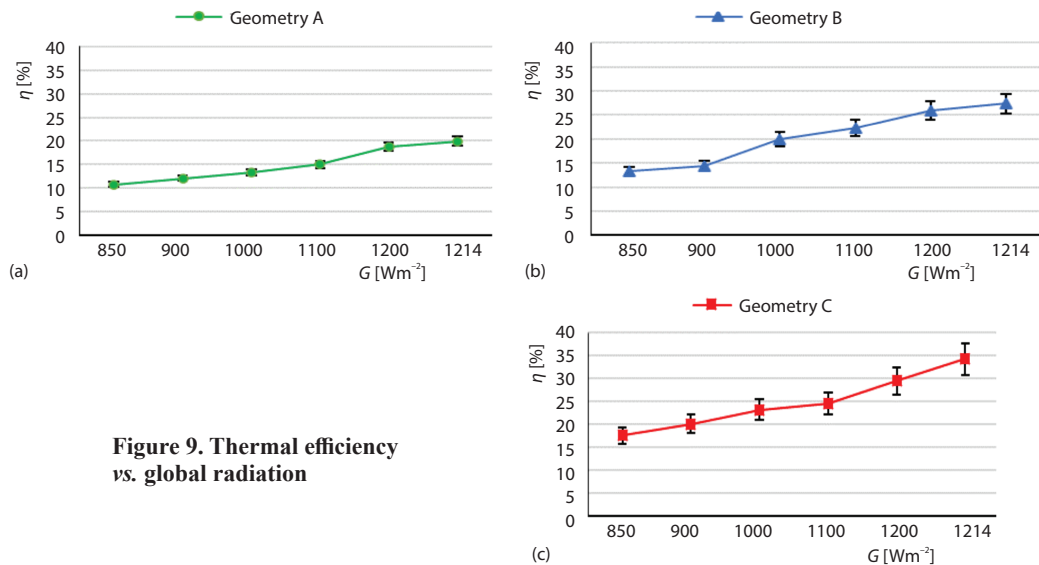


Figure 9. Thermal efficiency vs. global radiation

Analysis of reflective materials

After experimentation with different receiver geometries and attaining maximum performance from geometry C, the analysis was further extended by identifying the effects of different reflective materials. The reflective materials were selected based on solar weighted reflectance. Solar weighted reflectance is the crucial parameter to characterize the quality and performance of solar mirrors. It is the specular reflectance within a specified incidence and half-cone angle beam weighted across the solar spectrum. In this research two reflective materials of PTC namely: aluminum and austenitic polished stainless steel with mirror surface were selected. Radiant properties of selected reflector materials has been provided tab. 2 [30, 35, 36]. Performance assessment of both reflectors was carried under similar experimental conditions. Since geometry C was identified as the best receiver tube geometry, therefore, this geometry was used for further experimentation.

The average variation of optical efficiency with both reflector coatings (aluminum and stainless steel) during experimental days is shown in fig. 10. It can be observed from the figure that optical efficiency of aluminum coating ranged between 50-65%, whereas, optical efficiency of stainless steel reflector ranged between 30-55%. It must be noted that optical efficiency was higher than experimental thermal efficiency. This is due to the fact that the effects of all environmental conditions except clouds at fixed latitude are ignored in optical efficiency equation [36].

Table 2. Material properties

Parameter	Value
Absorptance of absorber, α	0.93
Transmittance of acrylic box, τ	0.93
Reflectivity of aluminum, ρ	0.94
Reflectivity of stainless steel, ρ	0.65
Instantaneous intercept factor, γ	0.95
Geometrical reduction factor, A_f	0.1

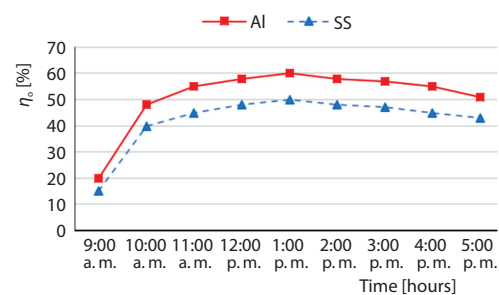


Figure 10. Optical efficiency of reflector coatings

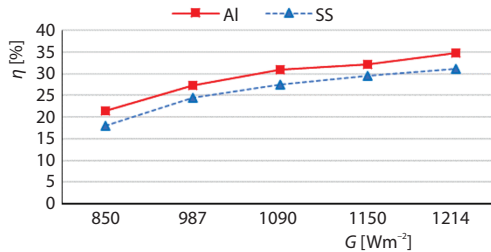


Figure 11. Thermal efficiency vs. global radiation

ing maximum efficiencies achieved for aluminum reflector and stainless steel reflector at this radiation were 34.8% and 31.04%, respectively. It is worthy to note that 12% higher thermal efficiency has been achieved from aluminum reflector as compared to stainless steel reflector.

Figure 11 illustrates the thermal efficiencies of selected materials at various global radiations. From figure, it can be observed that the thermal efficiencies of 21.45% and 18% were achieved for aluminum reflector and stainless steel reflector, respectively, at lowest global radiation of 850 W/m^2 . It can also be observed that thermal efficiency increased with increase in global radiation and become maximum at global radiation of 1214 W/m^2 . The correspond-

Conclusions

The objective of this work was to investigate the effects of innovative receiver geometries and reflective coatings on the performance of PTC. Three receiver geometries: simple tube (geometry A), receiver tube with straight absorber plate (geometry B), and receiver tube with curved absorber plate (geometry C) along-with two reflective materials aluminum and stainless steel (SS) were experimentally analyzed at specified location Taxila Pakistan. The most important findings of this work are given as follows.

- Geometry C resulted in better performance in terms of temperature variation ΔT , heat gain Q_{gain} and thermal efficiency as compared to geometry B and A.
- The results indicated that extended geometry is more sensitive to temperature variation which ultimately leads to higher performance. Since geometry C was attached with absorber plate having 50% additional cross-sectional area of receiver pipe, geometry B was in point contact with receiver pipe, whereas, geometry A had no absorber plate, therefore, geometry C outperformed geometry B and A.
- The comparative analysis presented aluminum reflector better than stainless steel reflector in terms of achieving higher thermal efficiency.

In future, there is need to research innovative geometries which increase the contact area without compromising the reflectivity of trough surface.

Nomenclature

A_{apr}	– aperture area of PTC, [m^2]
A_r	– surface area of receiver, [m^2]
A_f	– geometrical reduction factor
C_r	– concentration ratio
C_p	– specific heat, [$\text{Jkg}^{-1}\text{K}^{-1}$]
d_i	– inner diameter of receiver tube, [m]
d_o	– outer diameter of receiver tube, [m]
G	– global radiation, [W^{-2}]
L	– length of PTC, [m]
\dot{m}	– HTF mass-flow rate, [Ls^{-1}]
Q_{gain}	– theoretical useful heat gain, [W]
Q_{rad}	– heat transfer through radiation between the receiver and sky [W]
ΔT	– HTF temperature rise, [$^{\circ}\text{C}$]
T_{amb}	– ambient temperature, [$^{\circ}\text{C}$]

T_{in}	– inlet temperature of HTF, [$^{\circ}\text{C}$]
T_{out}	– outlet temperature of HTF, [$^{\circ}\text{C}$]
W_{apr}	– aperture width of PTC [m]

Greek symbols

α	– absorptance of receiver
γ	– instantaneous intercept factor
δ	– declination angle, [$^{\circ}$]
η	– thermal efficiency of system, [%]
η_o	– optical efficiency, [%]
θ	– angle of incidence, [$^{\circ}$]
θ_z	– zenith angle, [$^{\circ}$]
ρ	– trough reflectance
τ	– transmittance of absorber
ω	– solar Hour angle, [$^{\circ}$]

Acronyms

DAS – data acquisition system

HTF – heat transfer fluid

PTC – parabolic trough collector

References

- [1] Bellos, E., et al., Thermal Enhancement of Solar Parabolic trough Collectors by Using Nanofluids and Converging-Diverging Absorber Tube, *Renewable Energy*, 94 (2016), Aug., pp. 213-222
- [2] Azam, M., et al., *Sun Tracking Solar Panel System*, University of Delhi, Delhi, India, 2016
- [3] Chaudhry, M. A., et al., Renewable Energy Technologies in Pakistan: Prospects and Challenges, *Renewable and Sustainable Energy Reviews*, 13 (2009), 6-7, pp. 1657-1662
- [4] Adger, W. N., et al., Assessment of Adaptation Practices, Options, Constraints and Capacity, *Climate Change*, 200 (2007), Jan., pp. 719-743
- [5] ***, U.S.N.R.E.L.(NREL). Available from: http://www.nrel.gov/international/ra_pakistan.html
- [6] Kumaresan, G., et al., Performance Studies of a Solar Parabolic Trough Collector with a Thermal Energy Storage System, *Energy*, 47 (2012), 1, pp. 395-402
- [7] Fernández-García, A., et al., Parabolic-Trough Solar Collectors and their Applications, *Renewable Sustainable Energy Reviews*, 14 (2010), 7, pp. 1695-1721
- [8] Bellos, E., et al., Daily Performance of Parabolic trough Solar Collectors, *Solar Energy*, 158 (2017), Dec., pp. 663-678
- [9] Gandhi, A. S., et al., Comparative Study of Geometry of Receiver of Solar Parabolic Trough Concentrator, *International Journal of Recent Trends in Engineering & Research*, 2 (2016), 6, pp. 398-405
- [10] Han, H.-Z., et al., The RST Model for Turbulent Flow and Heat Transfer Mechanism in an Outward Convex Corrugated Tube, *Computers Fluids*, 91 (2014), Mar., pp. 107-129
- [11] Daabo, A. M., et al., The Optical Efficiency of Three Different Geometries of a Small Scale Cavity Receiver for Concentrated Solar Applications, *Applied Energy*, 179 (2016), Oct., pp. 1081-1096
- [12] Demagh, Y., et al., Numerical Investigation of a Novel Sinusoidal Tube Receiver for Parabolic trough Technology, *Applied Energy*, 218 (2018), May, pp. 494-510
- [13] Kumar, A., Shukla, S., Thermal Performance Analysis of Helical Coil Solar Cavity Receiver Based Parabolic trough Concentrator, *Thermal Science*, 23 (2019), 6A, pp. 3539-3550
- [14] Bellos, E., Tzivanidis, C. J. E., Enhancing the Performance of Evacuated and Non-Evacuated Parabolic trough Collectors Using Twisted Tape Inserts, Perforated Plate Inserts and Internally Finned Absorber, *Energies*, 11 (2018), 5, 1129
- [15] Jaramillo, O., et al., Parabolic trough Solar Collector for Low Enthalpy Processes: An Analysis of the Efficiency Enhancement by Using Twisted Tape Inserts, *Renewable Energy*, 93 (2016), Aug., pp. 125-141
- [16] Huang, Z., et al., Numerical Study on Heat Transfer Enhancement in a Receiver Tube of Parabolic trough Solar Collector with Dimples, Protrusions and Helical Fins, *Energy Procedia*, 69 (2015), May, pp. 1306-1316
- [17] Bellos, E., et al., Enhancing the Performance of Parabolic trough Collectors Using Nanofluids and Turbulators, *Renewable and Sustainable Energy Reviews*, 91 (2018), Aug., pp. 358-375
- [18] Razmmand, F., Mehdipour, R., Effects of Different Coatings on Thermal Stress of Solar Parabolic trough Collector Absorber in Direct Steam Generation Systems, *Thermal Science*, 23 (2019), 2, pp. 727-738
- [19] Medina Carril, D. M., et al., Finite Element Analysis of a Solar Collector Plate using Two Plate Geometries, *Ingenieria e Investigacion*, 36 (2016), 3, pp. 95-101
- [20] Duffie, J. A., Beckman, W. A., *Solar Engineering of Thermal Processes*, John Wiley & Sons, New York, USA, 2013
- [21] Kaczor, Z., et al., Numerical Studies on Capability to Focus Solar Radiation with Mirrors of Different Curvatures, *Thermal Science*, 23 (2019), Suppl. 4, pp. S1153-S1162
- [22] Sadaghiyani, O. K., et al., Two New Designs of Parabolic Solar Collectors, *Thermal Science*, 18 (2014), 2 pp. 323-334
- [23] Bellos, E., Tzivanidis, C., Enhancing the Performance of a Parabolic trough Collector with Combined Thermal and Optical Techniques, *Applied Thermal Engineering*, 164 (2020), 114496
- [24] Arasu, A.V., Sornakumar, S. T., Performance Characteristics of the Solar Parabolic trough Collector with Hot Water Generation System, *Thermal Science*, 10 (2006), 2, p. 167-174
- [25] Muthu, G., et al., Solar Parabolic Dish Thermoelectric Generator with Acrylic Cover, *Energy Procedia*, 54 (2014), Dec., pp. 2-10

- [26] Macedo-Valencia, J., *et al.*, Design, Construction and Evaluation of Parabolic Trough Collector as Demonstrative Prototype, *Energy Procedia*, 57 (2014), Dec., pp. 989-998
- [27] Noman, M., *et al.*, An Investigation of a Solar Cooker with Parabolic Trough Concentrator, *Case Studies in Thermal Engineering*, 14 (2019), 100436
- [28] Iqbal, W., *et al.*, Experimental and Theoretical Performance Investigation of Parabolic trough Collector for Industrial Sector in the Region of Taxila, *Technical Journal*, 25 (2020), 2
- [29] Harrison, P. G., *Chemistry of Tin*, Blackie Glasgow, Glasgow, UK, 1989
- [30] Tzivanidis, C., Bellos, E., The Use of Parabolic trough Collectors for Solar Cooling – A Case Study for Athens Climate, *Case Studies in Thermal Engineering*, 8 (2016), Sept., pp. 403-413
- [31] Kalogirou, S. A., Solar Thermal Collectors and Applications, *Progress in Energy and Combustion Science*, 30 (2004), 3, pp. 231-295
- [32] Duffie, J. A., Beckman, W. A., *Solar Engineering of Thermal Processes*, ed. 4th, John Wiley and Sons, New York, USA, 2013
- [33] Tzivanidis, C., *et al.*, Thermal and Optical Efficiency Investigation of a Parabolic trough Collector, *Case Studies in Thermal Engineering*, 6 (2015), Sept., pp. 226-237
- [34] Cengel, Y. A., Cimbala, J. M., *Fluid Mechanics*, Tata McGraw-Hill Education, New York, USA, 2006, Vol. 1
- [35] Fernandez-Garcia, A., *et al.*, Parabolic-trough Solar Collectors and Their Applications, *Renewable and Sustainable Energy Reviews*, 4 (2010), 7, pp. 1695-1721
- [36] Noman, M., *et al.*, An Investigation of a Solar Cooker with Parabolic trough Concentrator, *Case Studies in Thermal Engineering*, 14 (2019), 100436